Numerical Simulations of Radar Surface Air Pressure Measurements at O_2 Bands

Bing Lin and Yongxiang Hu

***Abstract* — An active microwave method is investigated for measuring surface air pressure by using radar reflections at frequencies around 53 ~ 55 GHz O_2 bands. The numerical simulation results for homogeneous backgrounds show that with an airborne radar working at these O_2 absorption bands, the rms errors of the radar surface pressure estimations with 15dB SNR can be as low as 4 ~ 7 mb. A radar system that covers these wavelengths will have great potentials for weather observations and other meteorological applications.**

***Index Terms*—Atmospheric Pressure, Differential Absorption Radar, Microwave remote sensing**

I. Introduction

Surface air pressure is one of the most important parameters regularly measured at surface meteorological stations. With developments of remote sensing methods, especially in airborne and satellite remote sensing techniques, large scale and global surface pressure measurements significantly lag other important parameters, such as surface temperature. There were some suggestions using satellite oxygen A-band methods (both passive and active) to measure the pressure ([1]~[4] and references therein). The active instruments rely on the operation of complicated highly stable laser systems on a space platform and are thus technically difficult, while passive methods are restricted to daytime measurements and areas of low cloud cover [1]. Thus, after about two decades of the suggestions, there are still no real remote sensing measurements of surface pressure, even in experimental stages.

This study considers active microwave techniques at strong O_2 absorption bands (around 50~56 GHz wavelengths) for the remote sensing of surface air pressure. At these frequencies, the total extinction of radar echoes from surfaces is strongly correlated with atmospheric column O_2 amounts, thus, atmospheric path lengths and surface air pressures. Flower and Peckham [5] studied the possibility of a microwave pressure sounder using active techniques. A total of six channels covering frequencies from ~25GHz to ~75GHz were considered. A major problem in this wide spectral region is the significant additional dependence on microwave absorption by liquid water (LW) clouds and atmospheric water vapor (WV). Atmospheric and cloud water temperatures also have different effects on the absorptions at different wavelengths. The complexity in even matching footprints of the six different wavelength channels makes this system difficult [1]. Here, we propose to use dual (or multiple) frequency O_2 band radar to overcome the above obstacles. The considered dual wavelength channels have very similar water vapor and liquid water absorption characteristics and footprints because of their close spectra. The microwave absorption effects due to LW and WV should be effectively removed from the ratio of reflected radar signals of the two channels. Simulations suggest that the accuracy of surface air pressure estimations from the ratio could reach 4 ~ 7mb, which is very useful for operational weather modeling and forecasting. The basic physical characteristics of O_2 band radar signals are discussed using a simplified analytic method in section 2 of this paper. Surface air pressure retrieving techniques are highlighted in these discussions. Theoretical methods to simulate O_2 band radar signals in both clear and cloudy weather conditions are introduced in section 3. The atmospheric profiles used in the simulations are from NOAA global radiosonde measurements. Section 4 presents simulated results of radar surface air pressure retrievals. Results show that radar O_2 absorption band techniques for surface air pressure remote sensing should meet basic meteorological requirements for operational weather forecasting. Conclusions of the advantage and disadvantage of the radar O_2 absorption band techniques are given in section 5. Within current developments of radar technology, it is possible that advanced O_2 differential absorption radars can be built and used in operational airborne weather remote sensing platforms.

2. Theoretical Basis of Surface Air Pressure Remote Sensing

This study serves as an initial investigation in surface pressure remote sensing. We are going to use a simplified radar signal propagation model to show the basic relationship between O_2 band radar reflected signals and surface pressure measurements in this current section. The actual simulations of radar reflected signals, which utilize complicated microwave radiative transfer (MWRT) calculations accounting for full physical processes of the radar signal propagation, will be discussed in the next section. This simplified model considers only atmospheric gas and cloud water absorptions and transmissions of radar signals to avoid the extreme complicity

Manuscript received Sept. 1, 2004. This research was sponsored by the NASA Earth Science Enterprise through the Clouds and Earth's Radiant Energy System (CERES) Mission and EOS science data analysis program.

Bing Lin is with NASA Langley Research Center, Science Directorate, Hampton, VA 23681 (phone: 757-864-9823; fax: 757-864-7595; e-mail: bing.lin-1@nasa.gov).

Yongxiang Hu is with NASA Langley Research Center, Science Directorate, Hampton, VA 23681 (e-mail: yongxiang.hu-1@nasa.gov).

of the radar signal propagation in various atmospheric and surface conditions. The temperature dependences of microwave absorptions and transmissions for cloud water and atmospheric gases are not included in the current discussion, but will be accounted for in the full MWRT simulations of the next section. Although it is a simple analysis of the radar signal propagation process, it will show the fundamental characteristics of the signals with surface pressure. The retrieval method, then, will be developed based upon these characteristics.

For initial theoretical considerations of air borne radar remote sensing technologies for surface air pressure measurements, we make a simple choice for radar system parameters. That is, the considered radar is assumed to work at the same wavelengths (frequencies: 50~56GHz) as those of existing passive O_2 band temperature sounders, such as the Advanced Microwave Sounding Unit (AMSU), except without the highest AMSU O_2 absorption channels for upper troposphere and stratosphere to avoid excessive attenuations. We will show later that the wavelengths around 53 ~ 55GHz are the best choices for O_2 band radars in surface air pressure measurements. The O_2 bands have been used in passive microwave remote sensing for more than two decades, and theoretical uncertainties of radiative transfer processes at the bands are generally small because of dominant line-by-line absorption characteristics and reasonably predictable line-broaden features of the O_2 microwave absorptions at the spectra ([6]~[8]). This selection of frequencies also provides strong contrasts for the reflected radar signals from different radar channels to differentiate atmospheric O_2 path lengths (or microwave optical depths of the atmospheric O_2 absorptions) and similar LW and WV absorption characteristics and spatial resolutions to remove these effects from the reflected radar signals. Since the optical depths at these wavelengths are proportional to atmospheric column O_2 amounts, surface pressure may be estimated from the O_2 amounts, especially when multiple channels are used. Table 1 lists the spectral information of considered surface pressure radar systems.

Table 1 Spectral characteristics of considered radar systems

Ch. No.	Pass-band center freq. (GHz)	bandwidth (MHz)	No. bands
1	50.300	161.14	1
2	52.800	380.520	1
3	53.596±0.115	168.20	2
4	54.400	380.54	1
5	54.940	380.56	1
6	55.500	310.34	1

Considering a radar with a transmitted power P_T at wavelength λ and antenna gain G, we obtain the power ΔPs reaching a small surface area Δa at the range R in the viewing angle θ as:

$$\Delta Ps = P_T\, G\, T(\lambda, \theta)\, \Delta a / (4\pi\, R^2(\theta)), \qquad (1)$$

where T is the atmospheric transmittance at the radar wavelength. The power ΔPr received by the radar receiver is:

$$\Delta P_r = \Delta Ps\sigma^0(\lambda, \theta)T(\lambda, \theta)A_e/(4\pi\, R^2(\theta))$$
$$= P_T G A_e T^2(\lambda, \theta)\sigma^0(\lambda, \theta)\Delta a/(4\pi R^2(\theta))^2, \qquad (2)$$

where A_e is the effective aperture of the antenna and equal to $\lambda^2 G/(4\pi)$, and σ^0 is the backscattering coefficient of the surface. The total power received by the receiver from all areas covered by radar illuminating angles Θ and Φ can be expressed as:

$$P_r(\lambda) = \frac{P_T G^2 \lambda^2 \sum T^2(\lambda,\phi,\varphi)\sigma^0(\lambda,\phi,\varphi)\Delta a}{(4\pi)^3 R^4(\theta)} = \frac{P_T G^2 \lambda^2 \sum T^2(\lambda,\phi,\varphi)\sigma^0(\lambda,\phi,\varphi)\Delta\phi\Delta\varphi}{(4\pi)^3 R^2(\theta)}, \qquad (3)$$

where the summation ($\sum$) of $\Delta\phi$ and $\Delta\varphi$ integrates over antenna illuminating angles Θ and Φ (or over the radar angular beam widths; note that the product of the angular beam widths Θ and Φ is decided by antenna gain, i.e., $\Theta\Phi = 4\pi/G$). When the radar angular beam widths Θ and Φ are small enough, the viewing angle θ and range R can be considered as constants for the integration over radar illuminated areas. Thus,

$$Pr(\lambda) = P_T G^2 \lambda^2 (4\pi)^{-3} T^2(\lambda, \theta)\sigma^0(\lambda, \theta)\Theta\Phi/R^2(\theta) \qquad (4)$$

or,

$$Pr(\lambda) = P_T A_e T^2(\lambda, \theta)\sigma^0(\lambda, \theta)/(4\pi R^2(\theta)). \qquad (4')$$

Eqs. 3 and 4 are generalized radar equations of area-extensive targets with simplified atmospheric radiative transfer processes. Since only parameters T, σ^0 and R in the equation 4 are related to environmental conditions, and the rest are associated with radar system designs, the Eq. 4 can be further simplified as:

$$P_r(\lambda) = C(\lambda)\, T^2(\lambda, \theta)\sigma^0(\lambda, \theta)/R^2(\theta), \qquad (5)$$

where $C(\lambda) = P_T A_e/4\pi$ is the radar system parameter varying with the radar wavelength. At nadir ($\theta = 0$), the radar equation can be further simplified as:

$$P_r(\lambda) = C(\lambda)\, T^2(\lambda)\sigma^0(\lambda)/R^2. \qquad (6)$$

Since in the absence of precipitation, atmospheric scattering effects on the radar signal propagation are negligible, the major atmospheric agents attenuating the radar signals are O_2, cloud liquid water, and water vapor. Thus,

$$T(\lambda) = \exp(-\tau_O - \tau_L - \tau_V) = \exp(-\alpha_O O - \alpha_L L - \alpha_V V), \qquad (7)$$

where wavelength dependent numbers τ_i and α_i are the atmospheric optical depth and effective absorption coefficient for the atmospheric agent i (i = O, L, or, V) at the radar wavelength, respectively, and O, L, and V are the atmospheric column O_2 amount, cloud liquid water path, and column water vapor, respectively. Note that α_O values are weakly dependent on atmospheric pressure and temperature. We assume these values are only functions of wavelengths to simplify current discussion, and will consider this and other radar signal propagation effects in the simulations of the next section..

In the atmosphere, O_2 is generally uniformly mixed with other gases. The column O_2 amount is proportion to column air mass, i.e., $O = M_O A$ where M_O is the mixing ratio of O_2 to total air, and A is the column air mass. Since $A = P_0/g$, where P_0 and g are the surface air pressure and the acceleration of the earth's gravity, respectively, Eq. 6 can be expressed as:

$$P_r(\lambda) = \frac{C(\lambda)\sigma^0(\lambda)}{R^2}\exp(-\frac{2\alpha_o M_o P_0}{g} - 2\alpha_L L - 2\alpha_v V). \quad (8)$$

When two radar channels with close enough wavelengths λ_1 and λ_2 such as those listed in Table 1 are used, the surface radar backscattering coefficient, liquid water absorption coefficients, and water vapor absorption coefficients are very similar. Then the ratio of the radar received powers from these two channels is:

$$\frac{P_r(\lambda_1)}{P_r(\lambda_2)} = \frac{C(\lambda_1)}{C(\lambda_2)}\exp[-\frac{2(\alpha_o(\lambda_1)-\alpha_o(\lambda_2))M_o P_0}{g}]. \quad (9)$$

This ratio is predominantly decided by the surface atmospheric pressure. The temperature and pressure dependences of the effective O_2 absorption coefficients have secondary influences on the spectrum power ratio. Rearranging Eq. 9, we have the surface air pressure as a function of the radar power ratio:

$$P_0 = \frac{0.5g}{[\alpha_o(\lambda_2) - \alpha_o(\lambda_1)]M_o}\ln[\frac{C(\lambda_2)P_r(\lambda_1)}{C(\lambda_1)P_r(\lambda_2)}] \quad (10)$$

or simply written as:

$$\begin{aligned} P_0 &= C_0(\lambda_1, \lambda_2) + C_1(\lambda_1, \lambda_2)\log_e(P_r(\lambda_1)P_r^{-1}(\lambda_2)) \\ &= C_0(\lambda_1, \lambda_2) + C_1(\lambda_1, \lambda_2)\,Ri(\lambda_1, \lambda_2), \end{aligned} \quad (11)$$

where C_0 and C_1 are the wavelength dependent coefficients of the relationship between the radar power ratio and surface air pressure, and can be estimated from the radar measurements or theoretical calculations of the radar system design. The $Ri(\lambda_1, \lambda_2)$ value is the logarithm of the radar power ratio at wavelengths λ_1 and λ_2 (hereafter called the differential absorption index). From Eq. 11, it can be seen that a very simple near-linear relationship between surface air pressure and the differential absorption index is expected from the O_2 band radar data. A linear regression retrieval method for surface pressure estimation is a straightforward result of current analysis. The simplified analysis used here highlights the basic physics of O_2 band surface air pressure remote sensing, and the fundamental characteristics of the considered radar are summarized in Eq. 11. The details in the radar signal simulation and transmission and retrieval accuracy will be discussed in the next section using a more comprehensive microwave radiative transfer model.

3. Simulation: Model and Results

The technique used to simulate the propagation of radar signals within the atmosphere is based on a plane-parallel, multiple layered atmospheric microwave radiative transfer (MWRT) model that has been used to determine cloud liquid water path, column water vapor, precipitation, land surface emissivity and other parameters over land and ocean ([9]~[14]). To avoid the complexities of microwave scattering by precipitating hydrometeors and surface backscattering, this study deals only with non-precipitating conditions and homogeneous backgrounds. Thus, transmission and absorption of radar signals within each atmospheric layer are the major radiative transfer processes considered in the model calculations. For the absorption process, this MWRT model carefully accounts for the temperature and pressure dependences of cloud water and atmospheric gas absorptions [14]. At microwave wavelengths, temperature dependences of gas and water absorptions are significant, and produce some difficulties for MWRT modeling. There are several models available to account for gas absorption, which differ mainly in their treatment of water vapor continuum absorption. The *Liebe* model ([15], i.e., MPM89) was used here. It yields results that differ negligibly from those of the *Rosenkranz* [16]) model at the O_2 bands. Liquid water absorption coefficients were calculated from the empirical water refractive index formulae of *Ray* [17], which agree well (relative differences < 5%) with those from *Liebe et al.* [18] for cloud water temperture > –15°C. For colder clouds, the uncertainties in the absorption coefficients could be larger by more than 15% [14] because of a lack of direct measurements of the refractive index.

Current MWRT model is consistent of 200 constant-thickness layers from surface to 40km. There is virtually no gas absorption above the modeled top-of-atmosphere (TOA) at our considered spectra. The atmospheric profiles of temperature, pressure, humidity and gas amount are obtained from NOAA 1988 (NOAA'88) global radiosonde measurements. This NOAA'88 data set is widely used in radiation simulations and satellite remote sensing (e.g., [19]) and covers both land and ocean. The data set has more than 5000 profiles, and about 1/3 of them are for cloudy skies. In cloudy cases, the NOAA'88 profiles can have up to two layers of clouds. Thus, the simulated results represent both clear and cloudy conditions. Since the model TOA (40km) height is much higher than that of radiosonde measurements, whenever there are no radiosonde upper atmospheric observations, interpolated climatological values of the upper atmosphere [20] are used. The weighting functions for the interpolation are decided from the surface air temperatures and pressures to meet the radiosonde measured weather conditions. In order to have large variations in surface air pressure, for each NOAA'88 measured profile, the surface pressure is randomly shifted by a Gaussian number with standard deviation 12mb, and the ratio of the shifted surface air pressure to the measured surface pressure is calculated. The atmospheric pressures in the measured profile above the surface are then adjusted to the values using the same ratio as that of the surface pressure.

The considered radar system is assumed to fly at 15km altitude with velocity ~200m/s, downward looking beam-width 3° angle (or footprint 785m) and narrowband channels as shown in Table 1. During our simulation, since all wavelengths used in the radar system are very close to each other, we assume the surface reflection (or σ^0) to be the same (11 dB) for all frequency channels [21]. As we have shown in the previous section, the absolute magnitude of the surface reflectivity is not very important for surface pressure estimation as long as the spectral dependence of σ^0 within the O_2 bands is negligible.

The simulated signals are analyzed in the form of relative received power (RRP), i.e., the ratio of the received and transmitted powers of the considered radar system. Since the system works at O_2 absorption bands, the relative received

powers are generally weak. Certain signal coding techniques for carrier frequencies, correlators for signal receiving and long-time (0.2s) averages of received powers are needed for the radar system. A common binary biphase pseudo random noise coding with ~1μs code chip may provide reasonable signal strengths for one bit of radar transmission.

The surface reflected radar signals, i.e. RRP values, used in this section are simulated through the complicated MWRT calculations discussed previously. With the RRP values, we calculate the radar differential absorption index discussed in the section 2. As shown in section 2, the index and surface air pressure have a near-linear relationship, which points out the basic directions for surface air pressure remote sensing.

Atmospheric extinctions (or attenuations) vary dramatically at the O_2 band radar frequencies listed in Table 1. The higher the frequency, the stronger the O_2 absorption are at these wavelengths. At the lowest frequency (50.3GHz), the atmospheric extinction optical depth is about 0.5, and at the highest frequency (55.5GHz), the optical depth goes up sharply to about 9. These two frequency represent the extreme ends of weak and strong, respectively, atmospheric O_2 absorption for our considered active microwave remote sensing of surface pressure. With a weak O_2 absorption (i.e., small optical depth) radar signals would have significant influence from environments, such as atmospheric water vapor, cloud water amount and atmospheric temperature profile. While the atmospheric O_2 absorption is too strong, most of radar-transmitted power would be attenuated, and small changes in surface air pressure (or column O_2 amount) would not produce significant differences in the received powers. Thus, wavelengths with moderate to reasonably strong O_2 absorptions in the atmosphere are expected to serve our purpose best.

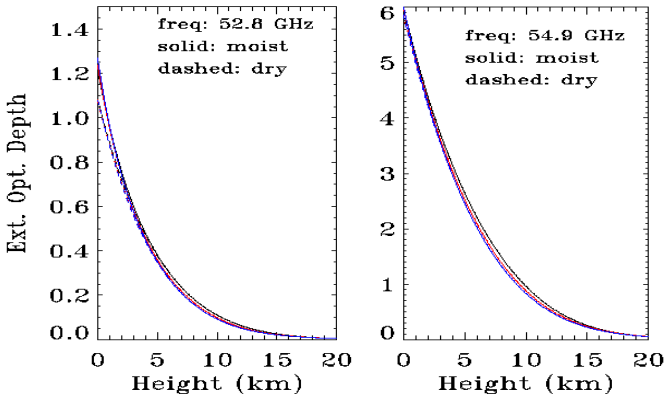

Figure 1 Atmospheric extinction optical depths for various atmospheric temperature and moisture at 52.8 (left) and 54.9 (right) GHz.

Figure 1 shows examples of atmospheric extinction optical depths counted from TOA under clear conditions using the standard profiles [20]. The three different color curves represent atmospheric surface temperatures of 280, 290 and 300K, respectively. It can be seen that these curves are very close to each other, indicating atmospheric temperature effects are minimal. For channel 2 (i.e. 52.8GHz, left panel) cases, the optical depths for moist atmospheres (solid curves) with 40mm column water vapor are about 1.25 and only 0.1 higher than those of dry atmospheres. At 54.9GHz (right panel), the optical depths are increased considerably to about 6, and different temperature and moist conditions have little effects on the total extinctions. For this frequency, the atmosphere extinctions of radar received signals due to double atmospheric path lengths reach about 50dB which requires some enhancements on radar signals to overcome system noise, as mentioned before. Generally, the atmospheric O_2 absorptions for channels 2 to 5 are at a reasonable level for surface pressure remote sensing. To test the accuracies of surface pressure measurements, a 15dB SNR (signal-to-noise ratio) is assumed for this primary study.

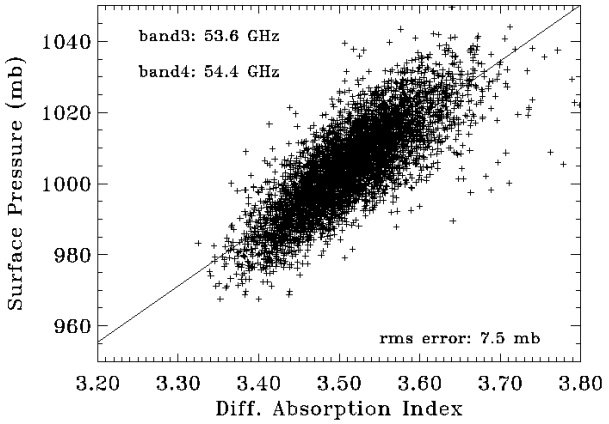

Figure 2 Simulated relationship between the differential absorption index, the logarithm of the radar spectrum ratio at wavelengths 53.6 and 54.4 GHz (or channels 3 and 4), and surface air pressure.

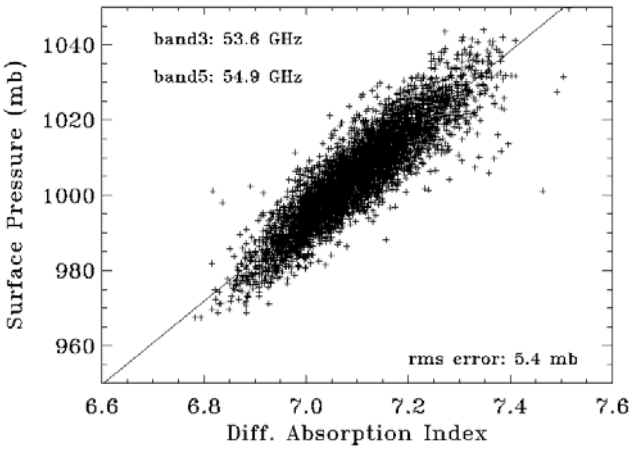

Figure 3 Similar as Fig. 2, except for 53.6 and 54.9 GHz.

Figure 2 shows the simulated relationship between the differential absorption index at wavelengths 53.6 and 54.4 GHz (or channels 3 and 4, respectively) and surface air pressure. Each point in the figure represents one adjusted NOAA'88 profile. As discussed in section 2, good linear correlations of the two variables are established with these simulations. A linear regression gives the root mean square (rms) error in

surface air pressure estimates about 7.5 mb, which may be suitable for normal meteorological uses. For channels 3 and 5 (Fig. 3), simulated results (5.4 mb) are close to current theoretical O_2 A-band results. The best results (Fig. 4) we found are those from the differential absorption index of channels 2 and 5. The rms error in this case is about 4.1 mb, which may be better than most proposed leading remote sensing techniques for surface air measurements. The tight linear relation between the surface air pressure and differential absorption index provides a great potential of remote sensing surface air pressure from airborne radar systems.

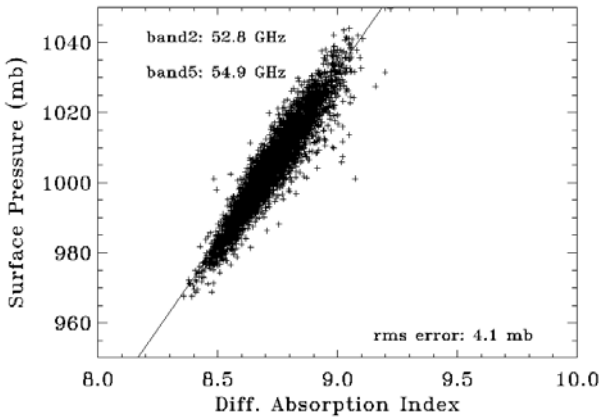

Figure 4 Same as Fig. 2, except for 52.8 and 54.9GHz.

4. Concluding Remarks

This study discusses a remote sensing method for surface air pressure. Primary results show that with an airborne radar working at about 53~55GHz O_2 absorption bands, the rms errors of the radar surface pressure estimations can be as small as 4~7mb under both clear and cloudy conditions. The considered radar systems should at least have 2 frequency channels to obtain the relative received power ratios of the two wavelengths. For the best simulated combination of 52.8 and 54.9 GHz channels, the power loss of radar received signals due to dual atmospheric path length absorptions could be as high as about 50 dB. High signal-to-noise ratios for radar reflected powers after these atmospheric absorptions can be achieved by using coded transmissions, correlators and long-time integration. The considered radar systems have great potentials for weather observations and numerical weather forecasts, especially over oceans. Future studies should focus on detailed radar system parameters and experimental tests of the radar systems to confirm current theoretical findings.

Acknowledgment

The authors would like to thank Alice Fan for her help in computer simulations and Dr. David Flittner for making the article more readable.

References

[1] Barton, I.J., and J.C. Scott, Remote measurement of surface pressure using absorption in the Oxygen A-band, Appl. Opt., 25, 3502-3507, 1986.

[2] Korb, C.L., and C.Y. Weng, A theoretical study of a two-wavelength lidar technique for the measurement of atmospheric temperature profiles', J. Appl. Meteorol., 21, 1346-1355, 1982.

[3] Singer, S.F., Measurement of atmospheric surface pressure with a satellite–borne laser, Appl. Opp. 7, 1125-1127, 1968.

[4] Wu, M.-L., Remote sensing of cloud top pressure using reflected Solar radiation in the Oxygen A-band, J. Clim. Appl. Meteor., 24, 539-546, 1985.

[5] Flower, D.A., and G.E. Peckham, A microwave pressure sounder, JPL Publication 78-68, CalTech, Pasadena, CA, 1978.

[6] Goldberg, M.D., Generation of retrieval products from AMSU-A: Methodology and validation, Tech. Proc. 10th TOVS Study Conf., Boulder, CO, Bureau of Meteorological research Centre, 215-229, 1999.

[7] Smith, W.L., H.M. Woolf, C.M. Hayden, D.Q. Wark, and L.M. McMillin, The TIROS-N operational vertical sounder, Bull. Amer. Meteor. Soc., 60, 1177-1187, 1979.

[8] Spencer, R.W., and J.R. Christy, Precision lower stratospheric temperature monitoring with the MSU: Technique, validation, and results 1979-1991, J. Climate, 6, 1194-1204, 1993.

[9] Lin, B., and W. B. Rossow, Seasonal variation of liquid and ice water path in non-precipitating clouds over oceans, *J. Clim., 9*, 2890-2902, 1996.

[10] Lin, B., and W. B. Rossow, Precipitation water path and rainfall rate estimates over oceans using Special Sensor Microwave Imager and International Satellite Cloud Climatology Project data, *J. Geophys. Res*., **102**, 9359-9374, 1997.

[11] Lin, B., B. Wielicki, P. Minnis, and W. Rossow, Estimation of water cloud properties from satellite microwave, infrared and visible measurements in oceanic environments, 1. Microwave brightness temperature simulations, *J. Geophys. Res., 103*, 3873-3886,1998a.

[12] Lin, B., P. Minnis, B. Wielicki, D. R. Doelling, R. Palikonda, D. F. Young, and T. Uttal, Estimation of water cloud properties from satellite microwave, infrared and visible measurements in oceanic environment, 2. Results, *J. Geophys. Res.,103*, 3887-3905,1998b.

[13] Lin, B. and P. Minnis, Temporal variations of land surface microwave emissivities over the ARM southern great plains site, J. App. Meteor., 39, 1103-1116, 2000.

[14] Lin, B., Patrick Minnis, Alice Fan, Judith A. Curry, and H. Gerber, Comparison of cloud liquid water paths derived from in situ and microwave radiometer data taken during the SHEBA/FIREACE, Geophys. Res. Letter, 28, 975-978, 2001.

[15] Liebe, H., MPM--An atmospheric millimeter-wave propagation model. *Int. J. Infrared and Millimeter Waves*, 10, 631-650, 1989.

[16] Rosenkranz, P., Water vapor microwave continuum absorption: A comparison of measurements and models, *Radio Sci*., 33, 919-928, 1998.

[17] Ray, P, Broadband complex refractive indices of ice and water, *Appl. Opt.*, 11, 1836-1844, 1972.

[18] Liebe, H., G. Hufford, and T. Manabe, A model for complex permittivity of water at frequencies below 1 THz, *Int. J. Infrared Millimeter Waves*, 12, 659-675, 1991.

[19] Seemann, S. W., J. Li, W. P. Menzel, and L. E. Gumley, Operational retrieval of atmospheric temperature, moisture, and ozone from MODIS infrared radiances, J. Appl. Meteorol., 42(8), 1072-1091, 2003.

[20] McClatchey, R., R. Fenn, J. Selby, E. Voltz, and J. Garing, Optical properties of the atmospheric, Air Force Cambridge Research Laboratories Environmental Research Paper AFCRL-72-0497, No. 411, 108pp, 1972.

[21] Callahan, P.S., C.S. Morris, and S.V. Hsiao, Comparison of TOPEX/POSEIDON σ_0 and significant wave height distributions to Geosat, J. Geophys. Res., 99, 25015-25024, 1994.